Expert Systems with Applications 38 (2011) 5584–5590

Contents lists available at ScienceDirect

Expert Systems with Applications

journal homepage: www.elsevier.com/locate/eswa

Design a breeze sensor system based on electric field via two-elemental direction

Wen-Tsai Sung *, Kuan-Yu Chen, Yao-Chi Hsu

Department of Electrical Engineering, National Chin-Yi University of Technology, No.35, Lane 215, Section 1, Chung-Shan Road, Taiping City, Taichung County 411, Taiwan

ARTICLE INFO

Keywords:
Electric field
Breeze sensing network
Wind speed
Measurement
Wireless sensors network

ABSTRACT

The research is mainly to design a portable anemometer that can display two-elemental direction and data as well as measure the variations of small wind speed and instantaneous wind speed based on wireless sensors network (WSN). The research principle is to use gas molecules of Negative high-voltage free air to form different equipotential field, which will offset as it's affected by wind, and the voltage differences measured by sensing bars of four terminals will be values of wind speed and wind direction. The circuit design of the research is to use piezoelectric transformer to generate negative high voltage with features of high efficiency, high step-up ratio and thinness and small size; and circuit board production is used by SMD parts with features of light weight, small size and portability. The experimental results demonstrate that two-elemental direction and value can be displayed at same time and the minimum value of wind speed can be less than 0.05 m/s. As compared with vane anemometer, it can measure the small wind that can be measured by rotary anemometer, thus the device of the experiment is demonstrated to be an anemometer that can measure two-elemental and small speed wind. The sensor of the research can sense air convention, gas emissions and gas leakage with wide range of applications such as in the industries of aerospace, energy and food, biochemical laboratory, hospital isolation room, office, storage facilities, mine field, tunnel, car and so on. In the future it can take integrated design to integrate the electric circuit into the IC and be applied in the MEMS to make measurements without external high voltage. It can make measurement for microsurgery and measure the flow of airflows of body organs by combining with biotechnology.

1. Introduction

The research principle is to use gas molecules of Negative high-voltage free air to form different equipotential field, which will offset as it's affected by wind, and the voltage differences measured by sensing bars of four terminals will be values of wind speed and wind direction. And I will observe whether the measurements on small wind are better than vane anemometer. The advantage of the two-elemental electric field anemometer is two-elemental structure, so it can measure direction and wind speed at same time. Its measured value can be less than 0.05/s with quick response and no movement inertia, and it can measure variations of instantaneous wind speed and be not easily affected by environment. In order to enhance set-up ratio, excellent efficiency, thinness and small size, it use piezoelectric transformer to generate negative high voltage. The production of circuit plate on the sensing terminal is made with SMD parts with features of small size and portability. It can sense air convention, gas emissions and gas leakage with wide range of applications such as in the industries of aerospace, energy and food, biochemical laboratory, hospital isolation room, office, storage facilities, mine field, tunnel, car and so on. Indoor anemometer must be light and small size, so the portability is the design direction of the research.

The anemometers currently available on the market can measure wind speed, but as for the smaller wind, it's difficult for them to measure. Taking vane anemometer as an example, too smaller wind can not move vane, thus it can not measure small wind; if we use hot wire anemometer to make measurement, the too small wind can not achieve effect of lowering temperature; furthermore the above two anemometers are ones can only make single direction measurement and the wind direction must be known before measurement, so the it's not convenient to make any measurement. Therefore, the focus of the research is to design an anemometer that can measure smaller wind speed as well as make multi-direction measurement.

2. Literatures review

For a survey on wind measurement in human history came very early. The Eastern Han Dynasty in AD 132, scientist Mr. Zhang Heng further presented the related issues in "copper bird with wind". He set straight upwards a 5-Zhang (about 11.5 meters) pole in a wide open ground and installed a rotary copper bird on the top of pole (Asano & Kinukawa, 1986). In 1797, a US meteorologist Mr.

* Corresponding author. Tel.: +886 4 23924505 7225; fax: +886 4 23924419.
E-mail addresses: songchen@ncut.edu.tw, songchen@ms10.hinet.net (W.-T. Sung).

0957-4174/$ - see front matter © 2010 Elsevier Ltd. All rights reserved.
doi:10.1016/j.eswa.2010.10.077

George E. Curtis made a double-feathered wind direction indicator, as a forerunner of anemometer to facilitate its swing in the breeze (Asano, Higashiyama, & Matsuzaka, 1988). In United Kingdom, Mr. Robinson first made a rotary cup anemometer in 1846. Richard Company in Paris made an Anemo-Cinemograph in 1887, which was the predecessor of propeller-type wind direction anemometer. British Mr. W. H. Dines invented a Dines anemometer in 1892 (Asano, Higashiyama, Yatsuzuka, & Urayama, 1990). In the field of upper-air observation, a non-staff balloon equipped with instruments was used in wind observation by the Blue Hill weather station in Milton in 1895. It could make observation in altitude as high as 18 km. Starting in 1925, airplane was used for the regular measurement of wind (Barat, 1982). Instruments were directly loaded in the plane for observation of the wind field. To convert wind power to turn the propellers of fan was used to measure speed of wind in 1965 (Cooley & Stever, 1952). Rotation speed and electric power generated by a small generator was calculated (Good, Brown, & Harpell, 1978). It took advantage of not being affected by electric and magnetic field of environment, simple in structure and, therefore low cost. It had several disadvantages of being restricted in single direction measurement, on-head area and position of rotors influencing the accuracy, rotors being stuck by moisture in tunnel, and being impossible for a very low speed measurement. Meanwhile, the inertia phenomena made it impossible to measure an instantaneous change. In 1973, a hot wire anemometer was first applied in laboratory. It mainly made use of an electrically heated thin platinum wire, placing in the air current to measure the wind speed by correlation with the intensity of heat loss of the wire. It had the advantage of usage in the turbulent environment (Chang, Kelly, & Crowley, 1995). In 1990, a one-elemental, ionic flow anemometer using high voltage pulse was developed in Japan (Melcher, 1981). The molecule of air was electrically activated in a fixed distance by high voltage pulse. It had the disadvantage that it could only make single direction measurement and the right direction should be obtained by trial-and-error, and more control electric circuit and better isolation measures needed to adopt as the wind became strong. Another one-elemental, fixed electric field, parallel polar plate measurement was applied in 1995 (Teager, 1980). It mainly applied high voltage between the polar plates to ionize the air molecule within it in a fixed distance. Recorded the time period of ionized air detected by the sensing terminal and calculated the wind speed by dividing the distance by time. The advantage was that it was small in size and saved electric energy as it needs less electric circuits to control high voltage. The disadvantage was that it could only make single direction measurement. It is a fundamental issue to choose the architecture for designing a fusion system. The usual architectures include the three traditional architectures introduced by Hall (1992). Hall's system did not provide any directions suitable for improving the efficiency of sensor fusion algorithms. This investigation implemented a two-elemental direction parallel data integrated system to improve the above wind measurement drawbacks. The data fusion approach employing two-elemental structure and High Voltage Generation Electric Circuit performed better than traditional methods in WSN system, network resources, measurement classification and global optima ability (Woodson & Melcher, 1968).

3. Breeze sensing network structure and methodology

3.1. Measurement on one-elemental electric field

Electric current is a coarse, average quantity that tells what is happening in an entire wire. Input two electrode plates in one conduit and connect with external high voltage to generate even electric field (shown as Fig. 1) and polarize the air. As opposite charges attract, so moving direction will be negative charges, if positive ions are implemented with force from polar Plate 1 to polar plate 2, the distribution of flow of charge is described by the current density (Yamanaka, Hirosawa, & Matsuzaka, 1985):

$$\vec{J}(r,t) = qn(m\vec{e}(r,t) + \vec{w}(r,t)) \tag{1}$$

where $J(r,t)$ is the current density vector at location r at time t, n is the particle density in count per volume at location r at time t, q is the charge of the individual particles with density qn is the charge density, m represents ion mobility, $\vec{e}(r,t)$ represents electric field, and $\vec{w}(r,t)$ represents wind speed (Nicules & Nath, 2003).

When no wind, arrival time of ion cloud from Plate 1 to Plate 2:

$$t_{No\text{-}wind} = \frac{d}{m\vec{e}} = \frac{d}{m\vec{V}} \tag{2}$$

When there is wind, arrival time of ion cloud from Plate 1 to Plate 2

$$t_{wind} = \frac{d}{m\vec{e} + \vec{w}} \tag{3}$$

$$\Delta t = t_{No\text{-}wind} - t_{wind} = \frac{d^3\vec{w}}{m^2\vec{v}^2} \tag{4}$$

From time difference, the wind speed is: (V is external voltage)

$$\vec{w} = \frac{\Delta t m^2 \vec{v}^2}{d^3} \tag{5}$$

The current received in the Plate 2 is: (A is cross-sectional area for conduit)

$$I_{No-wind} = Anqm\ \vec{e} = \frac{Anqm\ \vec{v}}{d} \tag{6}$$

When there is wind

$$I_{wind} = Anq\left(m\frac{\vec{v}}{d} + \vec{w}\right) \tag{7}$$

From current difference, the wind speed is

$$\vec{w} = \frac{I_{wind} - I_{No\text{-}wind}}{Anq} \tag{8}$$

3.2. Two-elemental electric field measurement

To change method of one-elemental fixing electric field parallel polar measurement into two-elemental structure, then it can measure two-elemental wind direction and wind speed. Because of high voltage, for safety, so the high voltage ends should be placed in the middle and protected with isolation net in the outer side that can prevent touching high voltage and disturbance of external signals. To measure voltage difference gains wind speed, wind direction and simultaneous variations. Fibrous wool is added in the middle to enhance electrostatic transduction and sensitivity. The design square figure of two-elemental electric field breeze anemometer is as Fig. 2 (Klein, 1993). Its principle mainly applies negative high voltage to ionize air to form charged ion cloud. When no wind, as the distribution of ion cloud is even, so the charges of 4

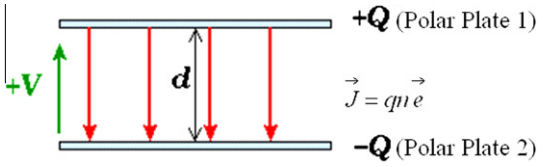

Fig. 1. One-elemental electric field.

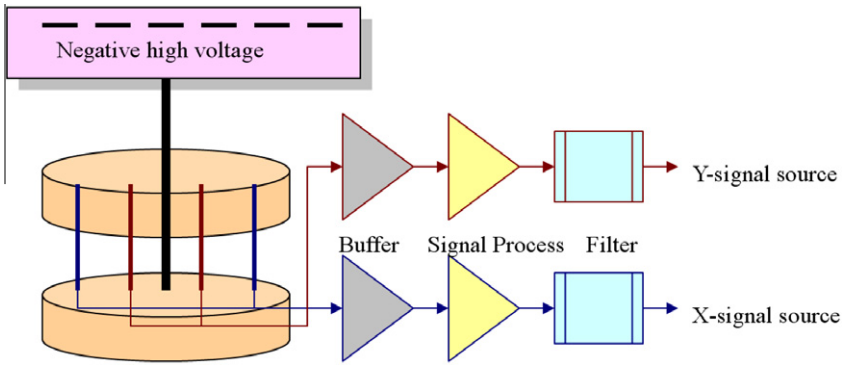

Fig. 2. Two-elemental electric field breeze anemometer.

receiving terminals are equal, as there is wind, the charges of 4 receiving terminals are not equal and converted into voltage through buffer amplifier and calculated through subtractor, finally output through filter and displayed with curve form in the *X* and *Y* axes. From the graph distribution, the values of wind direction and speed can be decided (Sun, Chen, Han, & Gerla, 2005).

3.3. Structure of two-elemental electric field breeze anemometer

The two-elemental structure is better than one-elemental in the Electromagnetism measurement because it can provide multi-signal source (Tian & Georganas, 2002). The one-elemental can only measure in single direction and wind direction shall be pre-known, so the measurement is very inconvenient; and the two-elemental structure can measure the speed wind as well as make multi-direction measurement. From the square figure of generating high voltage (Fig. 3(a)), square waves generated from oscillation circuit are output to step-up terminal through drive circuit, stepped up by piezoelectric transformer and output to be negative high voltage DC through voltage rectifier circuit. In the square figure of receiving end (Fig. 3(b)), as the action of negative high voltage, the air are ionized to form current that are converted to be voltage output in the buffer end and calculated different values through subtractor and amplified by amplifier for easy observation (Abrams, Goel, & Plotkin, 2004).

The experiment needs two groups of receiving end circuit and filter circuit with vertical placement of A_i, $-A_i$ and B_i, $-B_i$ of receiving end and input point of negative high voltage in the middle, which form two-elemental sensing circuit with following structure coordinates figure (Fig. 4a), the structure of peripheral isolation net is as (Fig. 4b), wind direction and speed can be calculated from the negative/positive values of A_{oo} and B_{oo} (Cardei, Thai, Li, & Wu, 2005).

4. System architecture

The sensor hardware design consists of four basic parts shown as Fig. 5. One WSN node device comprised sensing units, processing units, transceiver units and power units. In our research, we utilize wireless sensor network technique which is consisted of multi-device in particular area such as factories, houses, or even in large area such as freeway traffic systems, battlefields and mountains. ZigBee is a wireless protocol used by the IEEE 802.15.4 association and ZigBee alliance. The networks examined in this study are self-organized via the ZigBee wireless protocol. According to these features of technique, we adopt this technique to apply in our system. Besides, we also insert variety of sensors on the terminal of the system to monitor the information that we require (Shermer, 1992).

5. Experiment results and discussion

This study needs two power supplies, one oscilloscope, one wind speed generator, square working platform, high voltage circuit board, sensing circuit board, HV probe and vane anemometer. Fig. 6 indicated the experiment environment.

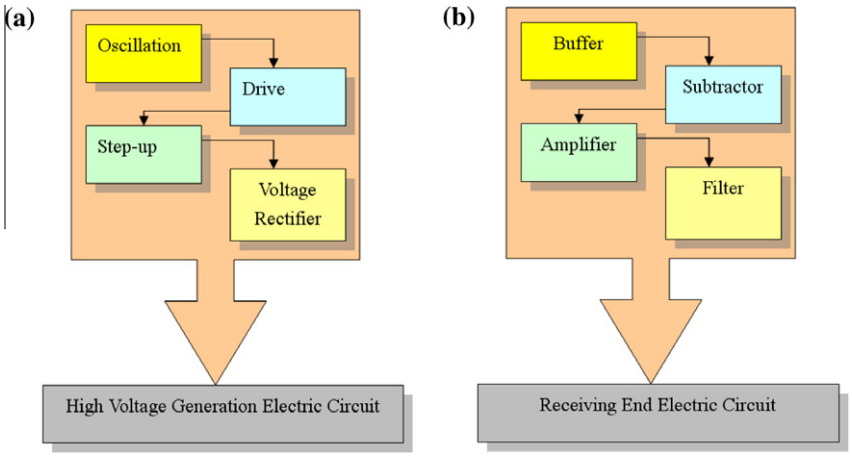

Fig. 3. (a) Flower charts on electric circuit of high voltage generation (b) and circuit of receiving end.

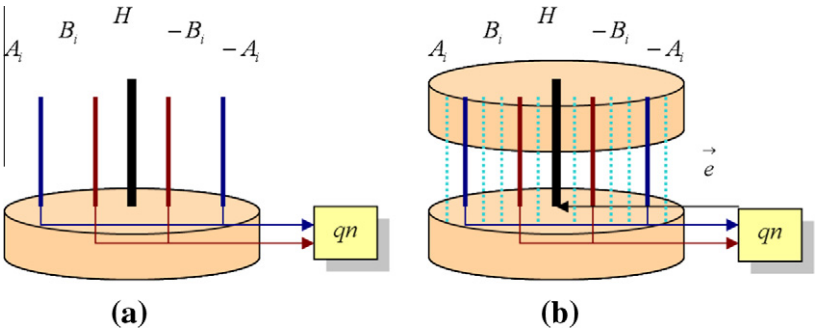

Fig. 4. (a) Two-elemental structure coordinates (b) integrated two-elemental sensing structure.

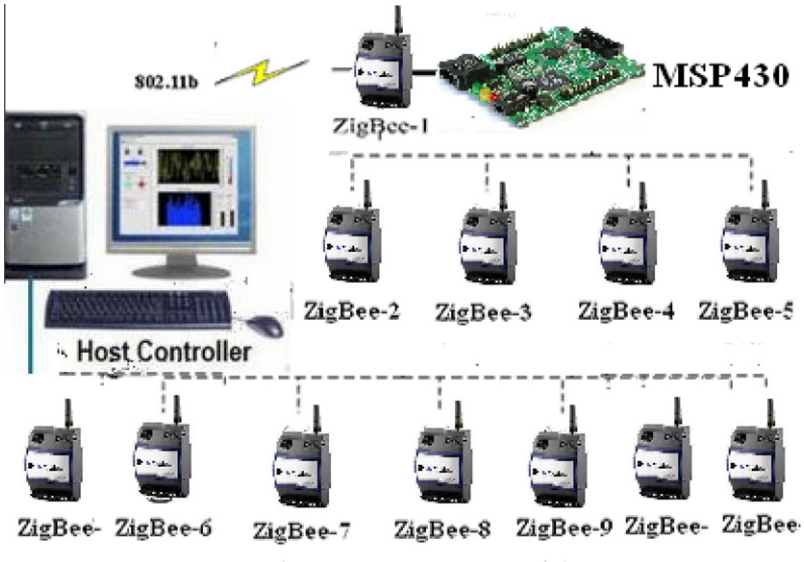

Fig. 5. System structure.

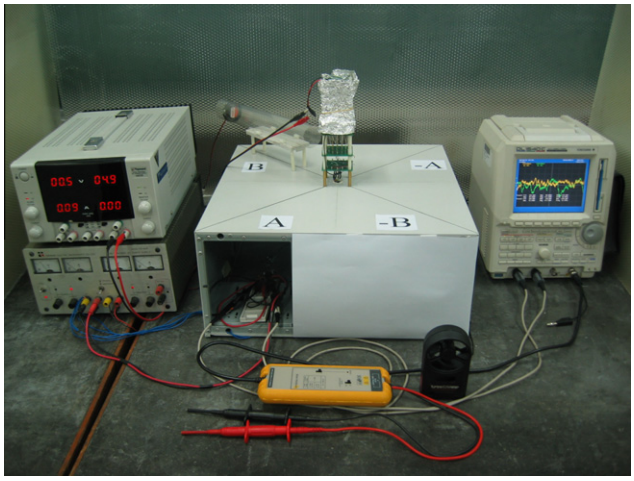

Fig. 6. Experiment environment.

5.1. Measurement principle

Generally to measure wind direction is described with 16 positions or 360°. The experiment, for measurement convenience, take A_i and $-A_i$ as X- axis and B_i and $-B_i$ as Y-axis, A_i as east, $-A_i$ as west, B_i as north and $-B_i$ as south. The experiment is executed under 4 conditions: no wind, wind from A-axis, wind from B-axis and wind between A- and B-axis. Equipotential line graph can be drawn according to the degree of air polarization. Central voltage of high voltage probe is highest and decreases slowly towards periphery. As the wind comes, the ion clouds will offset, so equipotential line will offset too, so wind direction and speed can be judged from offset direction and value.

5.2. Experiment results

The experiment is to gain different wind values by adjusting voltages of wind speed generator, and mainly makes measurements with 8 V input with oscilloscope displaying time-domain (10 ms/div) signal wave graph, among which the upper is A_o (200 mV/div) wave and lower B_o (200 mV/div) wave and its coordinate is shifted to be curves of X-axis and Y-axis. To observe the instaneous variations, X -axis is A_o (200 mV/div) and Y -axis B_o (200 mV/div) and makes further observation on the accumulated distribution map (30 s) (Adickes et al., 2002).

6. Measurement results analysis

6.1. Measurement on A-axis direction – The wind blows from A to −A in the experiment

Set wind speed generator as 8 V input, the time domain signal waveform will be as Fig. 7 (a), from which we know that signal

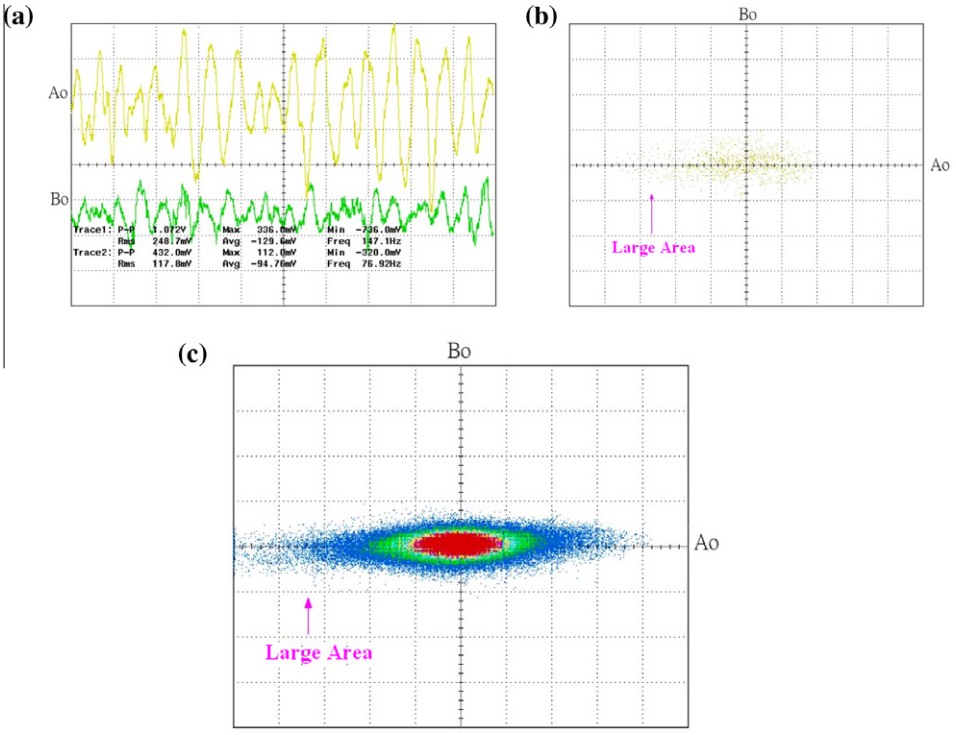

Fig. 7. (a) Time domain signal waveforms when 8 V wind blows towards $-A$ direction. (b) Instaneous coordinate changes map in X-axis and Y-axis when 8 V wind blows towards $-A$ direction. (c) Accumulated coordinate changes map in X-axis and Y-axis when 8 V wind blows towards $-A$ direction.

of A_o is bigger than B_o, and as the peaks variations of signal, we also can know the instaneous changes of wind speed. In coordinate curves of X-axis and Y-axis from A_o to B_o, instaneous changes map can be checked as Fig. 7 (b) and accumulated change map as Fig. 7(c). From the maps we can know that changes concentrated on the A_o-axis and area of $-A_o$ part is bigger, which demonstrates that equipotential line really deviates towards $-A$.

6.2. Make measurement in B-axis – The wind blows from B to −B in the experiment

Set wind speed generator as 12 V input, the time domain signal waveform will be as Fig. 8(a), from which we know that signal of B_o is bigger than A_o, and as the peak variations of signal, we also can know the instaneous changes of wind speed. In coordi-

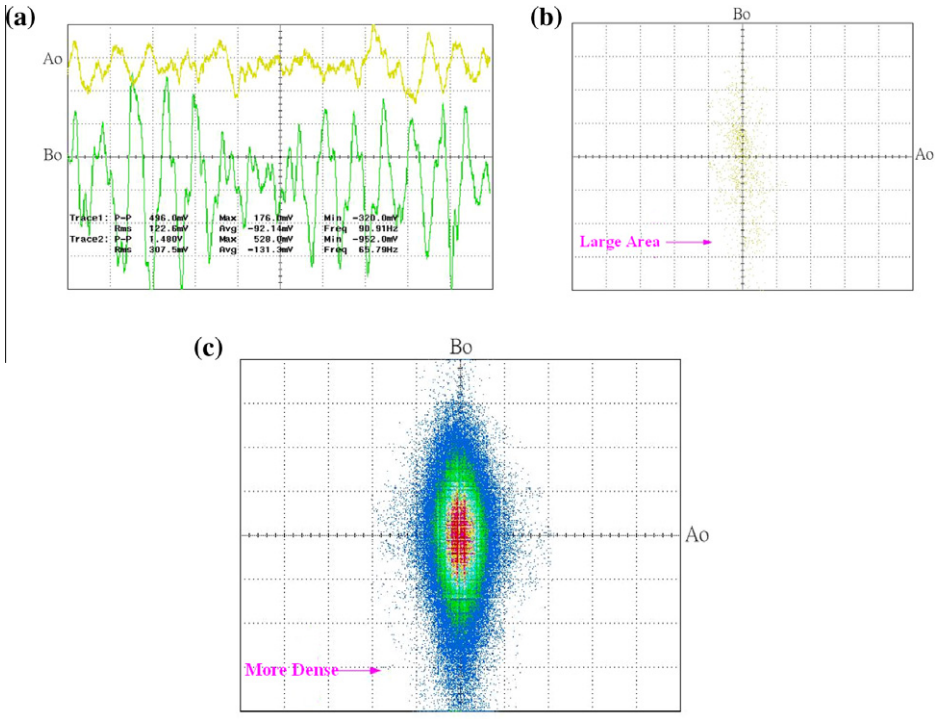

Fig. 8. (a) Time domain signal waveforms when 12 V wind blows towards $-B$ direction (b) instaneous coordinate changes map in X-axis and Y-axis when 8 V wind blows towards $-B$ direction (c) accumulated coordinate changes map in X-axis and Y-axis when 8 V wind blows towards $-B$ direction.

nate curves of *X*-axis and *Y*-axis from A_o to B_o, instaneous changes map can be checked as Fig. 8(b) and accumulated change map as Fig. 8(c). From the maps we can know that changes concentrated on the B_o-axis and area of $-B_o$ part is bigger, which demonstrates that equipotential line really deviates towards $-B$ (Tang, Man, & Ko, 1997).

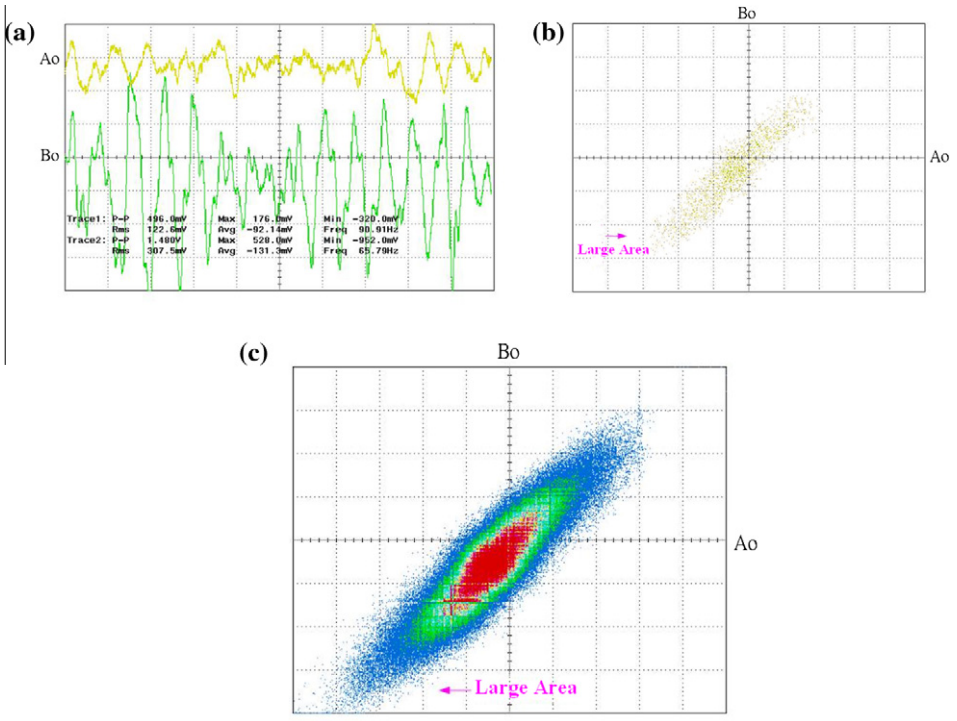

Fig. 9. (a) Time domain signal waveforms when 8 V wind blows towards direction of $-A$ and $-B$ direction (b) instaneous coordinate changes map in *X*-axis and *Y*-axis when 8 V wind blows towards $-A$ and $-B$ direction (c) accumlated coordinate changes map in *X*-axis and *Y*-axis when 8 V wind blows towards $-A$ and $-B$ direction.

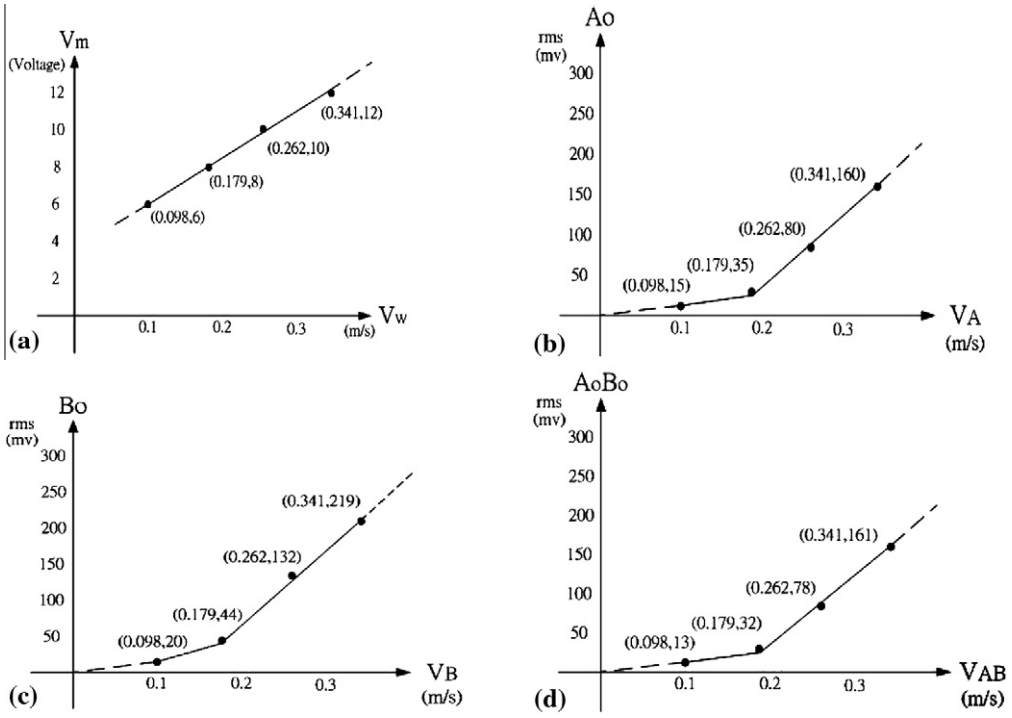

Fig. 10. (a) The relation between voltage of wind generator and wind speed (b) relation between wind speed and output voltage of A_o (c) relation between wind speed and output voltage of B_o (d) relation between wind speed and output voltage of A_oB_o.

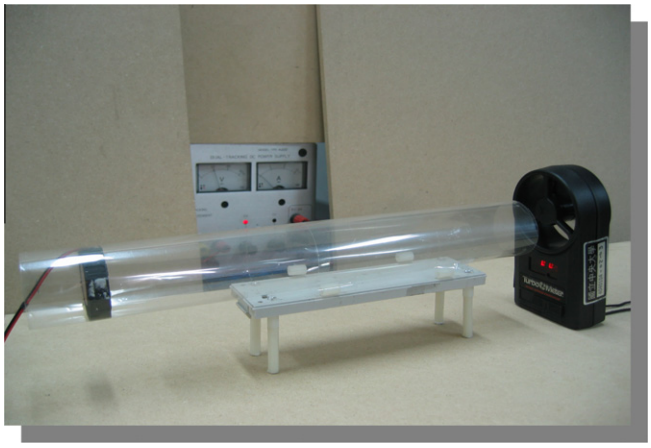

Fig. 11. Comparison map with vane anemometer.

6.3. Make measurement between A-axis and B-axis – The wind blows from AB to $-A-B$ in the experiment

Set wind speed generator as 12 V input, the time domain signal waveform will be as Fig. 9(a), from which we know that signal of A_o and B_o is similarly equal, and as the peak variations of signal, we also can know the instaneous changes of wind speed. In coordinate curves of *X*-axis and *Y*-axis from A_o to B_o, instaneous changes map can be checked as Fig. 9(b) and accumulated change map as Fig. 9(c). From the maps we can know that changes concentrated in the third quadrant and area of $-A_o$ and B_o part is bigger, which demonstrates that equipotential line really deviates towards direction of $-A$ and $-B$ (Raisanen, Whitaker, & Hurley, 2004).

The relation between wind generator voltage Vm and wind speed Vw is approximate linear relation as Fig. 10(a).

The relation of wind speed and output voltage of A_o is as Fig. 10(b), and the relation of wind speed and output voltage of B_o as Fig. 10(c), relation of wind speed and output voltage of A_oB_o is as Fig. 10(d), so from the output voltage value, we can know wind speed value. As wind speed is weaker the gravity, friction and viscosity of air molecules will more affect the air fluidity, so non-linear curve relationship is presented (Anderson & McGeehan, 1994).

The measurement scope of electric field anemometer is 0.08 m/s $\sim$ 20 m/s, and its comparison result with vane anemometer is as Fig. 11. AS set wind generator 8 V input, vane anemometer will not turn, therefore it demonstrates that two-elemental anemometer can measure the small wind that vane anemometer can not measure (Dhillon & Chakrabarty, 2003).

7. Conclusions and future work

The research characteristic is to use negative high voltage to ionize air and to know wind direction and speed through the variations of voltage on the induction terminal. As air ionization, so it has very sensitive induction capacity and can sense very small variations of wind, and as its two-elemental structure, it can make measurement without pre-known wind direction, therefore it's very convenient to make measurement. In order to achieve excellent step-up efficiency and light weight, piezoelectric transformer is applied to be as step-up material.

In general, sensors and posting information are usually operating in computers. In Our research and experiment, we improve some drawbacks such as PC has huge volume or space, thus, we use embedded platform to instead. Nowadays, although there are a lot of industrial monitor management systems on market, the common disadvantage is expensive and no feedback signal to main control end, hence, this reason makes most of system operate with low accuracy and time-delay. In our study, we use posting calculate chip and ZigBee wireless sensor detecting technique to establish discrete management web node, and connect with MSP430 embedded host which furnishes all kinds of information for each sensor and processes in time. Therefore, it is solve the problem of positing sensors and also decrease the cost in our platform.

Acknowledgements

This research was supported by the National Science Council of Taiwan under grant NSC 99-2220-E-167-001. The authors thank the National Chin-Yi University of Technology, Taiwan for financially supporting this research.

References

Abrams, Z., Goel, A., & Plotkin, S. (2004). Set k-cover algorithms for energy efficient monitoring in wireless sensor networks. In *Proceedings of IEEE third international symposium on information processing in sensor networks (IPSN '04)*, (pp. 424–432).

Adickes, M. D., Billo, R. E., Norman, B. A., Banerjee, S., Nnaji, B. O., & Rajgopal, J. (2002). Optimization of indoor wireless communication network layouts. *IIE Transactions, 34*(9), 823–836.

Anderson, H.R., & McGeehan, J.P. (1994). Optimizing microcell base station locations using simulated annealing techniques. In *Proceedings of IEEE 44th vehicular technology conference (VTC '94)*, (pp. 858–862).

Asano, K., Higashiyama, K., & Matsuzaka, Y. (1988). Fundamental characteristics of cage type ion-flow anemometer. *Proceedings of the Institute of Electrostatics Japan, 12*(6), 441–449.

Asano, K., Higashiyama, Y., Yatsuzuka, K., & Urayama, K. (1990). Ion-flow anemometer using high-voltage pulse. *IEEE IAS Conference, 1*, 802–808.

Asano, K., & Kinukawa, T. (1986). On the study of a differential type ion-flow anemometer. *Proceedings of the Institute of Electrostatics Japan, 10*, 123–130.

Barat, J. (1982). A high-resolution ionic anemometer for boundary-layer measurements. *Journal of Applied Meteorology, 21*, 1480–1488.

Cardei, M., Thai, M. T., Li, Y., & Wu, W. (2005). Energy-efficient target coverage in wireless sensor networks. *Proceedings of IEEE INFOCOM*, 1976–1984.

Chang, Jen-Shih, Kelly, Arnold J., & Crowley, Joseph M. (1995). *Handbook of electrostatic processes*. New York, Basel, Hong Kong: Marcel Dekker, Inc..

Cooley, W. C., & Stever, H. G. (1952). Determination of air velocity by ion transit-time measurements. *Review of Scientific Instruments, 23*, 151–154.

Dhillon, S.S., & Chakrabarty, K. (2003). Sensor placement for effective coverage and surveillance in distributed sensor networks. In *Proceedings of IEEE wireless communications and networking conference (WCNC '03)*, (pp. 1609–1614).

Good, R. E., Brown, J. H., & Harpell, G. (1978). Development of a corona anemometer for measurement of stratospheric turbulence. *AFGL-IP-265*.

Hall, D. L. (1992). *Mathematical techniques in multisensor data fusion*. Mass: Artech House.

Klein, L. A. (1993). A boolean algebra approach to multiple sensor voting fusion. *IEEE Transactions on Aerospace and Electronic Systems, 29*(2), 317–327.

Melcher, J. R. (1981). *Continuum electromechanics*. Cambridge, Mass, Sec. 5.5: MIT Press.

Nicules, D., & Nath, B. (2003). Ad-hoc positioning system (APS) using AoA. In *Proceedings of IEEE INFOCOM*, (pp. 1734–1743).

Raisanen, L., Whitaker, R.M., & Hurley, S. (2004). A comparison of randomized and evolutionary approaches for optimizing base station site selection. In *Proceedings of ACM symposium on applied computing (SAC '04)*, (pp. 1159–1165).

Shermer, T. C. (1992). Recent results in art galleries. *Proceedings of IEEE, 80*(9), 1384–1399.

Sun, T., Chen, L.J., Han, C.C., & Gerla, M. (2005). Reliable sensor networks for planet exploration. In *Proceedings of IEEE international conference on networking, sensing and control*, (pp. 816–821).

Tang, K.S., Man, K.F., & Ko, K.T. (1997). Wireless LAN design using hierarchical genetic algorithm. In *Proceedings of seventh international conference on genetic algorithm*, (pp. 629–635).

Teager, H. (1980). Some observations on oral air flow during phonation. *IEEE transactions on acoustics, speech, and signal processing, 28*, 599–601.

Tian, D., & Georganas, N.D. (2002). A coverage-preserving node scheduling scheme for large wireless sensor networks. In *Proceedings of ACM first international workshop on wireless sensor networks and applications (WSNA '02)*, (pp. 32–41).

Woodson, H. H., & Melcher, J. R. (1968). *Electomechanical Dynamics*. New York: John Wiley. Part 3, pp. 776–783.

Yamanaka, M. D., Hirosawa, H., & Matsuzaka, Y. (1985). Glow-discharge ionic anemometer. *Review of Scientific Instruments, 56*(4), 617–622.